The Journal of Immunology

Peptide Vaccines of the HER-2/*neu* Dimerization Loop Are Effective in Inhibiting Mammary Tumor Growth In Vivo

Stephanie D. Allen, Joan T. Garrett, Sharad V. Rawale, Audra L. Jones, Gary Phillips, Guido Forni, John C. Morris, Robert G. Oshima and Pravin T. P. Kaumaya

J Immunol 2007; 179:472-482; ;
doi: 10.4049/jimmunol.179.1.472
http://www.jimmunol.org/content/179/1/472

The Journal of Immunology is published twice each month by
The American Association of Immunologists, Inc.,
1451 Rockville Pike, Suite 650, Rockville, MD 20852

Print ISSN: 0022-1767 Online ISSN: 1550-6606.

Peptide Vaccines of the HER-2/*neu* Dimerization Loop Are Effective in Inhibiting Mammary Tumor Growth In Vivo[1]

Stephanie D. Allen,[2]*† Joan T. Garrett,[2]†‡ Sharad V. Rawale,† Audra L. Jones,§ Gary Phillips,¶ Guido Forni,‖ John C. Morris,# Robert G. Oshima, and Pravin T. P. Kaumaya[3]*†‡††**

Human epidermal growth factor receptor-2 (HER-2)/*neu* (ErbB2), a member of the epidermal growth factor family of receptors, is overexpressed in 20–30% of breast cancers. It is an attractive target for receptor-directed antitumor therapy using mAbs. Unlike other epidermal growth factor receptor family members, HER-2/*neu* does not bind a high-affinity ligand, but rather functions as the preferred dimerization partner. Pertuzumab (Omnitarg) is a humanized mAb directed against the HER-2/*neu* dimerization domain that inhibits receptor signaling. The recent definition of the crystal structure of the HER-2/*neu*-pertuzumab complex demonstrated that the receptor dimerization region encompassed residues 266–333. Based on the three-dimensional structure of the complex, we have designed three conformational peptide constructs (sequences 266–296, 298–333, and 315–333) to mimic regions of the dimerization loop of the receptor and to characterize their in vitro and in vivo antitumor efficacy. All the constructs elicited high-affinity peptide Abs that inhibited multiple signaling pathways including HER-2/*neu*-specific inhibition of cellular proliferation and cytoplasmic receptor domain phosphorylation. All the peptide Abs showed Ab-dependent cellular cytotoxicity to varying degrees with the 266–296 constructs being equally effective as compared with Herceptin. The 266–296 peptide vaccine had statistically reduced tumor onset in both transplantable tumor models (FVB/n and BALB/c) and significant reduction in tumor development in two transgenic mouse tumor models (BALB-*neu*T and VEGF$^{+/-}$Neu2–5$^{+/-}$). The 266–296 construct represents the most promising candidate for antitumor vaccination and could also be used to treat a variety of cancers with either normal or elevated expression of HER-2 including breast, lung, ovarian, and prostate. ***The Journal of Immunology,*** **2007, 179: 472–482.**

The human epidermal growth factor receptor-2 (HER-2)[4]/*neu* (ErbB2) tumor Ag is a member of the epidermal growth factor family of tyrosine kinase receptors (1). A ligand for HER-2/*neu* is unknown, but it appears to be the preferred dimerization partner for other members of the ErbB family. Homo- or heterodimerization of family members results in transphosphorylation of the intracellular tyrosine kinase domains and signal transduction (2–4). HER-2/*neu* overexpression has been demonstrated in a number of human tumors including 20–30% of breast cancers and is associated with aggressive disease and a worse prognosis (5–7). HER-2/*neu* is a well-established target for both passive and active immunization. mAbs, such as the humanized Ab trastuzumab (Herceptin), has been shown to induce tumor responses in 15–40% breast cancer patients whose tumors overexpress HER-2/*neu* (8). A second HER-2/*neu*-directed humanized mAb, pertuzumab (Omnitarg), has been developed (9) and has shown efficacy in non-HER-2/*neu* overexpressing tumors by interfering with multiple HER-2/*neu*-mediated signaling pathways (10). Recent phase I clinical trials demonstrated that pertuzumab was well-tolerated and clinically active (11, 12).

Despite impressive clinical results with anti-HER-2 mAb therapy and other Ab therapeutics, there are several drawbacks including severe side effects such as cardiocytotoxicity that have been observed in some patients (13). Given that Abs represent a growing class of human therapeutics, their use is as yet, rarely, if ever completely curative. Thus, there is considerable interest in developing both a prophylactic and therapeutic vaccine that could mediate antitumor activity, have sustained immune responses, and exhibit little toxicity with lower associated costs. Indeed, patients have shown the ability to mount weak humoral and cellular immune responses against HER-2/*neu* (14, 15). Both HER-2/*neu*-specific CTL and IgG Abs directed against HER-2/*neu* have been detected in 30–50% of breast cancer patients (16, 17), indicating that it is possible to break tolerance and mount an immune response against the HER-2/*neu* receptor (18, 19). Our laboratory proposed using B cell peptide epitopes as candidate HER-2/*neu* vaccines and developed several epitopes by mapping regions in the extracellular domain using computer-aided analysis (20, 21). Two HER-2/*neu* epitopes 628–647 and 316–339 were identified as viable candidates for active immunotherapy and these are presently being studied in a phase I trial.

The structure determination of the HER-2/pertuzumab Fab complex showing the complexity of the binding site (residues 266–333) provides considerable insights for the development of new vaccine candidates (22). Pertuzumab binds to the dimerization loop of subdomain II of the extracellular domain (ECD), blocking receptor

*Ohio State Biochemistry Program, †Department of Obstetrics and Gynecology, ‡Chemistry-Biology Interface Program, §Biochemistry Department, ¶Center for Biostatistics, The Ohio State University, Columbus, OH 43210; ‖Department of Clinical and Biological Sciences, University of Turin, Turin, Italy; #Metabolism Branch, Center for Cancer Research, National Cancer Institute, Bethesda, MD 20892; **Oncodevelopmental Biology Program, Burnham Institute for Medical Research, La Jolla, CA 92037; and ††Arthur G. James Comprehensive Cancer Center, The Ohio State University, Columbus, OH 43210

Received for publication February 27, 2007. Accepted for publication April 26, 2007.

The costs of publication of this article were defrayed in part by the payment of page charges. This article must therefore be hereby marked *advertisement* in accordance with 18 U.S.C. Section 1734 solely to indicate this fact.

[1] This work was supported by National Cancer Institute Grant 84356 (to P.T.P.K.).

[2] S.D.A. and J.T.G. contributed equally.

[3] Address correspondence and reprint requests to Dr. Pravin T. P. Kaumaya, The Ohio State University, Suite 316 Medical Research Facility, 420 West 12th Avenue, Columbus, OH 43210. E-mail address: Kaumaya.1@osu.edu

[4] Abbreviations used in this paper: HER-2, human epidermal growth factor receptor-2; Cyc, cyclized; NC, noncyclized; ADCC, Ab-dependent cellular cytotoxicity; HRG, Heregulin; MVF, measles virus fusion protein; ECD, extracellular domain; VEGF, vascular endothelial growth factor.

Table I. *Amino acid sequence of peptide vaccine constructs*

Designation[a]	Peptide	Sequence[b]
MVF 266 CYC	266–296 peptide with one disulfide bond	H_2N-*KLLSLIKGVIVHRLEGVE*-GPSL-LHCPA LVTYNTDTFESMPNPEGRYTFGASCV–COOH
MVF 298 CYC	298–333 peptide with two disulfide bonds	H_2N-*KLLSLIKGVIVHRLEGVE*-GPSL-ACPYNYLSTDVGSCTLVCPLHNQEVTAEDGTQRCEK-COOH
MVF 315 CYC	315–333 peptide with one disulfide bond	H_2N-*KLLSLIKGVIVHRLEGVE*-GPSL-CPLHNQEVTAEDGTQRCEK-COOH

[a] Peptides containing disulfide bonds (CYC) are shown; NC peptides are free peptides without disulfide bonds (not shown in table).
[b] MVF sequence is italicized and cysteine residues are underlined to indicate the locations of the disulfide bonds. Residues in bold indicate individual amino acids which directly contact pertuzumab (<3.2 Å distance).

dimerization and signal transduction independent of HER-2/*neu* overexpression. As a strategy to minimally dissect the conformational preference of this region, we selected and designed several peptides spanning sequences 266–296, 298–333, and 315–333 that overlap the pertuzumab-binding site on the dimerization loop.

In this study, we report on the activity of several constructs containing complex, differential disulfide pairings (Table I) as well as their linear counterparts to determine the best mimic of the pertuzumab-binding conformational region which can result in an effective vaccine that could be translated to the clinic. The immunogenicity of each cyclized (CYC) and noncyclized (NC) construct was determined in both mice and rabbits, eliciting a high-affinity, high-titer Ab response. All the Abs raised against the peptide constructs recognized the native HER-2/*neu* receptor with varying degrees of reactivity. The ability of the 266–296 peptide constructs to elicit the highest titer Abs, highest recognition of native HER-2 by showing a greater shift by FACS analysis comparable to trastuzumab, indicates that this sequence was the most immunogenic. Additionally, three of the six putative conformational constructs, 266CYC, 266NC, and 315CYC, were able to mediate Ab-dependent cellular cytotoxicity (ADCC) and reduce phosphorylation of the HER-2/*neu* tyrosine kinase domain. Importantly, epitope 266–296 was able to suppress cellular proliferation in heregulin (HRG)-stimulated MCF-7 cells. Our results show that the 266–296 pertuzumab-like epitope constructs had statistically reduced tumor onset in both transplantable tumor models (FVB/n and BALB/c) and significant reduction in tumor development in two transgenic mouse tumor models (BALB-*neu*T and VEGF$^{+/-}$Neu2–5$^{+/-}$). These studies demonstrate that both the linear (NC) and conformational (CYC) peptide vaccines corresponding to residues 266–296 of the dimerization region of HER-2/*neu* are able to elicit an immune response with antitumor capabilities, resulting in a peptide vaccine that will be able to mimic the effects of pertuzumab in vivo without the harmful side effects associated with mAb therapy.

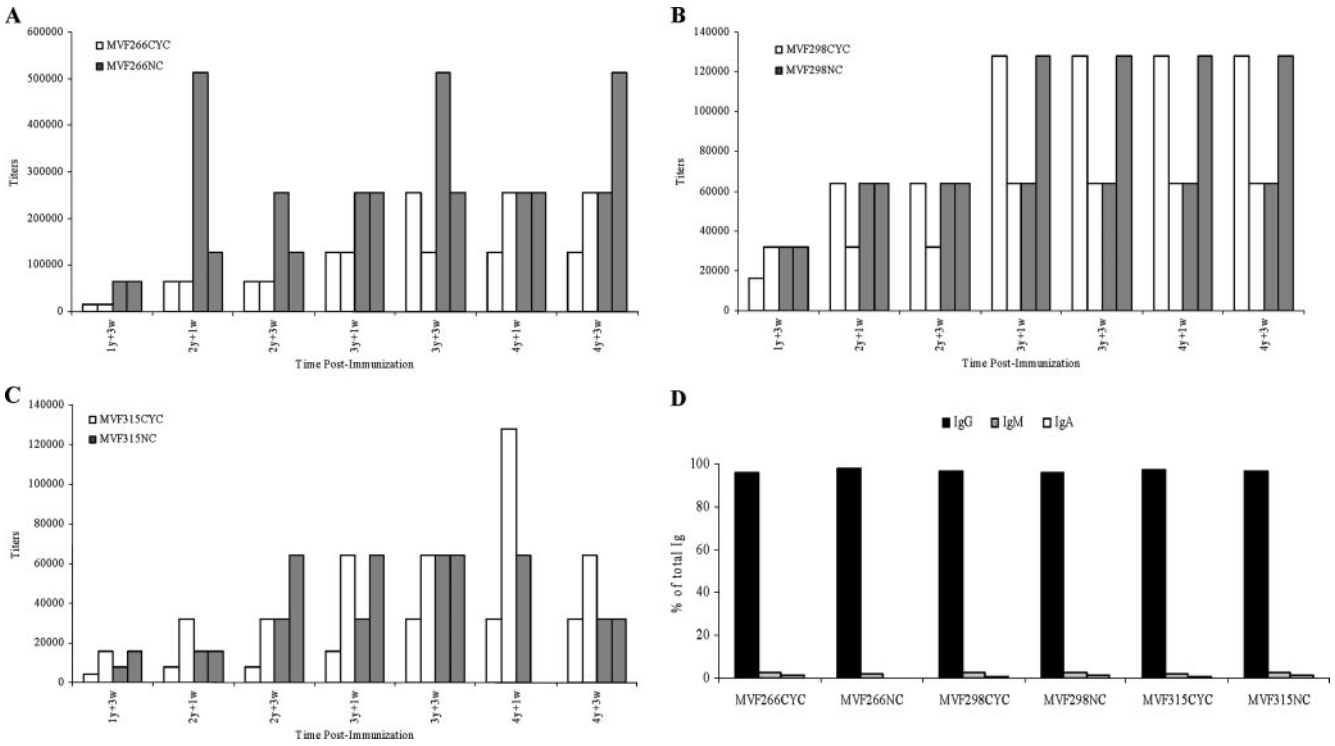

FIGURE 1. Ab responses elicited by peptide vaccines in outbred rabbits. Two rabbits per group were immunized (as described in *Materials and Methods*) with each vaccine construct for a total of four injections. Blood was drawn weekly and sera surveyed for peptide-specific Abs by ELISA. Each bar represents one rabbit. Titers are defined as the reciprocal of the highest serum dilution with an absorbance of 0.2 or greater after subtracting the background. 2y + 3w indicates the Ab titer in blood drawn 3 wk (3w) after the second immunization (2y). □, Cyclized peptide immunization; ▨, NC peptide immunization. *A*, Rabbits immunized with the MVF266 constructs. *B*, Rabbits immunized with the MVF298 constructs. *C*, Rabbits immunized with the MVF315 constructs. *D*, The levels of IgG, IgM, and IgA were determined for pooled sera obtained 2 wk after the third immunization for each peptide construct. The *y*-axis represents the percentage of total Ig.

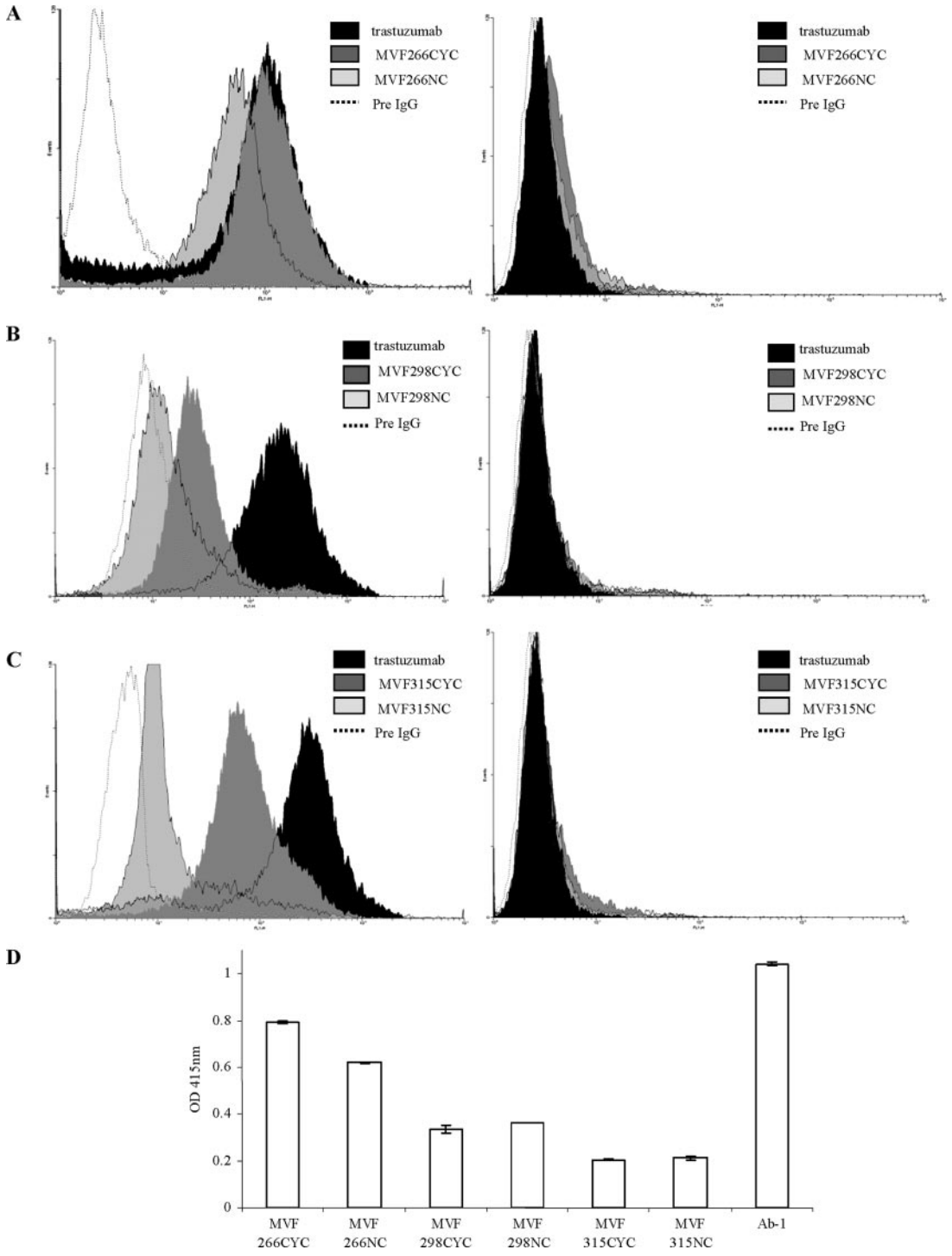

FIGURE 2. Cross-reactivity of the antipeptide Abs to native HER-2/*neu*. Flow cytometry was used to assess the binding capabilities of the antipeptide Abs to the native receptor. Purified Abs (5 μg) from immunized rabbit sera were tested against BT474 (HER-2^{high}) and MDA468 (HER-2^{low}) breast cancer cells. Histograms contain overlays of rabbit preimmunization IgG (negative control, dotted line), peptide Abs (CYC, dark gray shading; NC, light gray shading), and trastuzumab (5 μg, positive control, black shading). Ab binding was detected by goat-anti-rabbit FITC-conjugated secondary Abs. The *x*-axis represents fluorescent intensity and the *y*-axis represents relative cell number. *A*, Binding of MVF266CYC and MVF266NC Abs to BT474 (*left panel*) and MDA468 (*right panel*). *B*, Binding of MVF298CYC and MVF298NC Abs to BT474 (*left panel*) and MDA468 (*right panel*). *C*, Binding of MVF315CYC and MVF315NC Abs to BT474 (*left panel*) and MDA468 (*right panel*). *D*, Binding of antipeptide Abs to cellular lysate of SKBR-3 (HER-2^{high}) cells as measured by indirect ELISA. Reported as averages ± SEM.

Materials and Methods

Cell lines and Abs

All culture medium, FCS, and supplements were purchased from Invitrogen Life Technologies. The human breast cancer cell lines BT474, SKBR-3 (HER-2^{high}; ~20 × 10^6 molecules/cell), and MCF-7 (HER-2^{low}; ~10,000–50,000 molecules/cell) were purchased from American Type Culture Collection and maintained according to the supplier's guidelines. Mouse breast tumor cell lines NT2.5 were gifts from Drs. R. Todd Reilly, Johns Hopkins Medical School, Baltimore, MD. Ab-1, a rabbit polyclonal Ab that binds the kinase

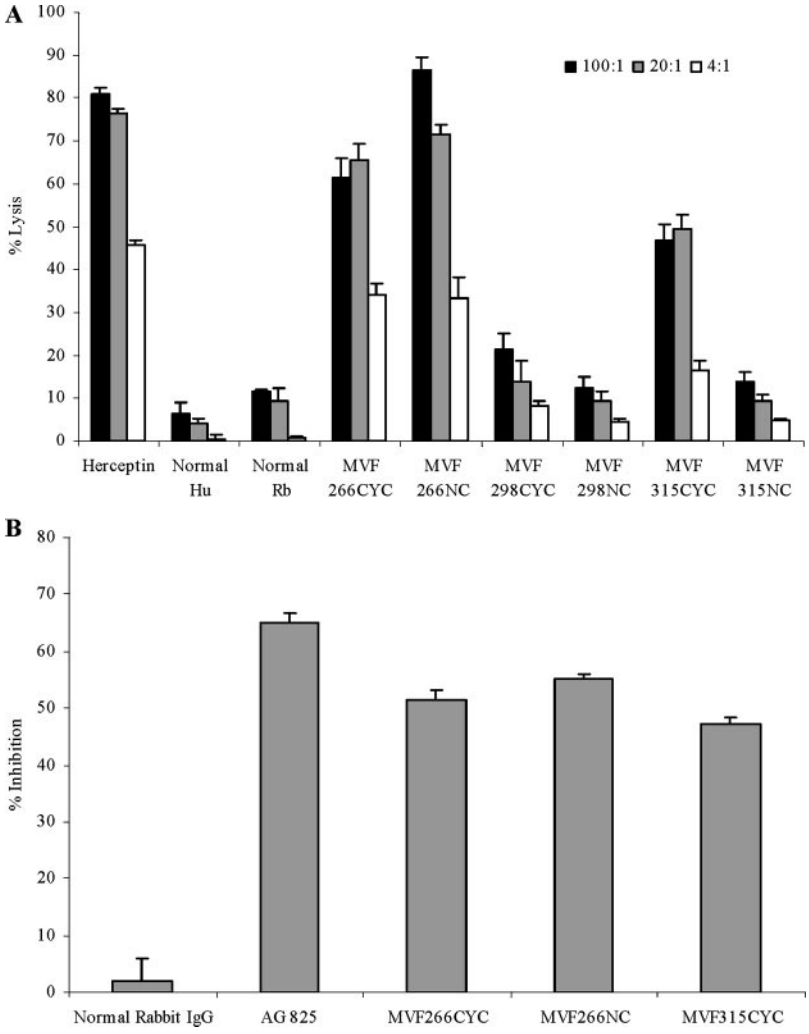

FIGURE 3. Anti-peptide Abs mediate ADCC and decrease cytoplasmic phosphorylation in vitro. *A*, Target cell line BT474 was coated with 50 μg of purified anti-peptide Abs from rabbits, normal rabbit IgG, normal human IgG (negative controls), or trastuzumab (positive control), then cultured in the presence of human PBMC effector cells to give an E:T ratio of 100:1, 20:1, and 4:1 in triplicates. Results are representative results of three experiments, ± SEM. *B*, SKBR-3 cells were incubated with 50 μg of MVF266CYC, MVF266NC, and MVF315CYC purified Abs before being exposed to HRG (HER-3 activating ligand) for 10 min, and lysed. Phosphorylated HER-2/*neu* was determined by indirect ELISA, and percent inhibition were calculated as in proliferation assay. Normal rabbit IgG was used as the negative control, and the phosphorylation inhibitor AG825 was used as the postive control. Representative results are shown ± SEM.

domain of HER-2, Ab-4, a mouse mAb that binds the extracellular domain of *neu*, and AG825 a HER-2 phosphorylation inhibitor was purchased from Calbiochem.

Animals

Female New Zealand White rabbits, FVB/n, and BALB/c mice were purchased from Harlan Breeders. Virgin female BALB-*neu*T mice (23) were generated by breeding wild-type (wt) BALB/c females with heterozygous BALB-*neu*T males. VEGF$^{+/-}$Neu2–5$^{+/-}$ bitransgenic mice were generated by crossing male MMTV-Neu2–5 mice (24) with female MMTV-VEGF-164 mice as described previously (25). Animal care and use was in accordance with institutional guidelines.

Synthesis and characterization of conformational and linear peptides

HER-2/*neu* B cell epitopes 266–296, 298–333, and 315–333 were colinearly synthesized with a promiscuous Th cell epitope derived from the measles virus fusion protein (MVF; residues 288–302) using a four residue linker (GPSL). Peptide synthesis was performed on a Milligen/Biosearch 9600 peptide solid-phase synthesizer using F-moc/t-butyl chemistry as previously described (26). Trt was used as side chain sulfhydryl protection for the 266 and 315 epitopes and double protection for 298 included Trt on Cys^{315} and Cys^{331} and Acm on Cys^{299} and Cys^{311}. Peptides were cleaved from the resin using cleavage reagent B (trifluoroacetic acid:phenol:water: TIS, 90:4:4:2), and crude peptides purified by semipreparative reversed-phase-HPLC and characterized by electrospray ionization mass spectroscopy (27). Intramolecular disulfide bonds were formed using iodine oxidation as described (28) and disulfide bridge formation was further confirmed by maleimide-PEO$_2$-biotin reaction and subsequent analysis using electrospray ionization mass spectroscopy.

Circular dichroism (CD) measurements

Aqueous solutions for CD were prepared by dissolving the freeze-dried peptide in appropriate amount of water to give final concentration of 0.5 mM and used as stock solution for further dilution. CD spectra were recorded on an AVIV model 62A DS CD instrument as reported earlier (26). Mean residue ellipticity ($[\theta]_{M,\lambda}$) values were calculated according to the equation, $[\theta]_{M,\lambda} = (\theta \times 100 \times M_r)/(n \times c \times l)$. Where θ is the recorded ellipticity (degree); M_r the m.w. of the peptide; n, the number of residues in the peptide; c, the peptide concentration (milligrams per milliliter); and l, the path length of the cuvette. Helicity of peptides was determined according to Chen et al. (29) with reference to mean residue ellipticity of polylysine for 100% α-helix $(\theta)_{222} = -35{,}700$ (30).

Active immunization of rabbits and mice

New Zealand White rabbits were immunized with 1 mg of peptide dissolved in ddH_2O emulsified (1:1) in Montanide ISA720 vehicle (Seppic) with 100 μg of *N*-acetylglucosamine-3yl-acetyl-l-alanyl-d-isoglutamine (nor-MDP). Mice, 6–8 wk old, were immunized with 0.1 mg of peptide emulsified in ISA720 with 100 μg of nor-MDP. Rabbits and mice were boosted with the respective doses at 3-wk intervals. Blood was collected via the central auricular artery in rabbits and retro-orbital sinus in mice and sera tested for Ab titers.

BALB-*neu*T mice (5–6 wk old) were immunized as described above. After the third vaccination, the BALB-*neu*T mice received boosters at monthly intervals. Mice were euthanized at 25 wk of age.

Passive immunization of VEGF$^{+/-}$Neu2–5$^{+/-}$ mice

VEGF$^{+/-}$Neu2–5$^{+/-}$ mice were treated with 750 μg of anti-peptide Abs twice weekly for 4 wk starting at 4 wk of age. Mice were monitored twice

weekly from days 45 to 67 for the development of palpable tumors. Average day of tumor onset was 56 days.

Ab purification

As described previously (26).

ELISAS

Ab titers were determined as previously described (20) and is defined as the reciprocal of the highest serum dilution with an absorbance of 0.2 or greater after subtracting background.

Isotype ELISA. Mouse serum was isotyped using Mouse Typer SubIsotyping kit (Bio-Rad) which was used per manufacturer's instructions.

HER-2 ELISA. Plates were coated overnight at 4°C with 100 μl of 10 μg/ml trastuzumab (Herceptin; Genetech), washed four times with 0.1% Tween 20/PBS, and blocked with of 100 μl of PBS-1% BSA 4 h. Plates were washed four times with 0.1% Tween 20/PBS. Wells were coated overnight at 4°C with 50 μl of either PBS-1% BSA or SK-BR-3 cell lysate (1×10^8 cells in 20 ml of lysis buffer (1% Triton X-100, 10% glycerol, 150 mM NaCl, 50 mM HEPES, 1.5 mM $MgCl_2$, 1 mM EDTA, 10 mM pyrophosphate, 100 mM NaF, 0.2 mM Na_3VO_4, 10 μg/ml aprotinin, 10 μg/ml leupeptin, 1 mM PMSF)). Plates were washed four times with 0.1% Tween 20/PBS, a 1/100 dilution of rabbit sera added, and incubated 2 h on a rocker. Ab binding was detected using goat-anti-rabbit IgG HRP.

Flow cytometry

BT474 (1×10^6) cells were incubated with anti-peptide Abs in 100 μl of 2% FCS in PBS for 2 h at 4°C. Normal rabbit IgG was used as a negative control and humanized trastuzumab used as a positive control. Unbound Abs were removed with PBS, and the cells incubated with FITC-conjugated anti-rabbit Abs for 30 min at 4°C in 100 μl of 2% FCS in PBS. Cells were washed in PBS and fixed in 1% formaldehyde before being analyzed by Coulter ELITE flow cytometer (Coulter). A total of 10,000 cells were counted for each sample. Debris, cell clusters, and dead cells were gated out by light scatter assessment before single parameter histograms were drawn and smoothed.

ADCC

As described previously (26). Briefly, 1×10^6 BT474 cells were incubated with 50 μg of anti-peptide Ab and 100 μCi of $Na^{51}CrO_4$ for 1 h at 37°C. Unbound Ab and excess chromium was removed and the cells added to human PBMCs and incubated 4 h at 37°C. Cell-free supernatant was collected and the release of chromium by lysed cells measured using a scintillation counter. Percent lysis = 100 × (experimental − spontaneous lysis)/(maximum lysis − spontaneous lysis).

Phosphorylation assay

A total of 1×10^6 SKBR-3 cells/well were plated in 6-well plates and incubated at 37°C overnight. Culture medium was removed and the cell layer washed once with PBS low score (% fcs). Culture medium was added to the wells and plates incubated overnight at 37°C. Cells were washed and 50 μg of Ab in binding buffer (0.2% w/v BSA, RPMI 1640 medium with 10 mM HEPES (pH 7.2)) was added to the wells and incubated at room temperature 1 h. HRG (5 nM/well) was added and the incubation continued at room temperature for 10 min. Binding buffer was removed and the cell layer washed once with PBS before adding 1 ml of lysis buffer (1% Nonidet P40, 20 mM Tris (pH 8.0), 137 mM NaCl, 10% glycerol, 2 mM EDTA, 1 mM Na_3VO_4, 10 μg/ml aprotinin, 10 μg/ml leupeptin). Plates were rocked at 4°C for 30 min. Lysates were removed, spun at 13,000 × *g* and supernatants collected. Protein concentration of each sample was measured by Coomassie plus protein assay reagent kit and lysates were stored at −80°C. Phosphorylation was determined by DuoSet IC for human phospho-ErbB2 according to the manufacturer's directions (R&D Systems).

Proliferation assay

MCF-7 cells (1×10^4) were plated in 96-well flat-bottom plates overnight. Growth medium was replaced with low sera (1% FCS) medium and the cells were incubated overnight. Media were removed from the wells and replaced with Ab in 1% medium. Plates were incubated for 1 h at 37°C before 10 ng/ml HRG was added in 1% medium. Plates were incubated an additional 72 h at 37°C before adding 5 mg/ml MTT to each well. Plates were incubated 2 h at 37°C, before adding 100 μl of extraction buffer (20% SDS, 50% dimethylformamide (pH 4.7)). Plates incubated overnight at 37°C and read on an ELISA reader at 570 nm with 655 nm background subtraction. Percent lysis = 100× (HRG-treated cells − Ab-treated cells)/(HRG-treated cells).

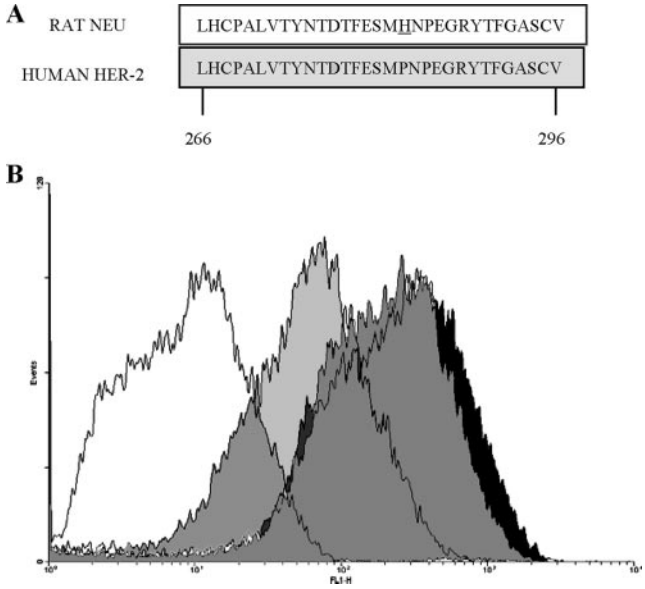

FIGURE 4. Cross-reactivity of the MVF266 anti-peptide Abs to rat *neu*. *A*, The amino acid sequences of rat *neu* (*top*) and human HER-2 (*bottom*, light gray shading) were aligned between human HER-2 sequence 266–296. *Neu* disparate residues are underlined. *B*, Flow cytometric analysis was performed on the NT2.5 cell line using 5 μg of Abs. Histograms indicate MVF266NC Abs (light gray shading), MVF266CYC (dark gray shading), normal rabbit IgG (negative control, dotted line histogram), and Ab-4 (anti-*neu* Ab, black shading).

Tumor challenge

NT2.5. Ten days after the third immunization, FVB/n mice were challenged with 3×10^6 NT2.5 cells. Mice were monitored twice weekly for the presence of palpable tumors for a total of 24 days.

TUBO. Fourteen days after the third immunization, BALB/c mice were challenged with 1×10^5 TUBO cells. Mice were monitored twice weekly for the presence of palpable tumors for a total of 39 days.

Tumor measurements

Tumor challenge. Palpable tumors were measured in a blinded fashion with Vernier calipers and tumor volume calculated by the formula (length × width^2)/2.

Transgenic tumors. Tumors in each of 10 mammary glands were measured for tumor volume as described above. Results for BALB-*neu*T are reported as total mean tumor volume per group and $VEGF^{+/-}Neu2\text{–}5^{+/-}$ results are reported as the average of the single largest tumor per mouse (25).

Statistical analysis

Tumor growth over time was analyzed using Stata's XTGEE (cross-sectional generalized estimating equations) model which fits general linear models that allow you to specify within animal correlation structure in data involving repeated measures. The model includes terms for treatment group, time, and the interaction of treatment by time. This interaction term is used to calculate the differences in the slopes of each group. The XTGEE model assumes that the data are normally distributed and that volume is a continuous linear variable. Log transformation of the volume addresses both of these issues. The slopes by treatment of the log-transformed tumor volumes were calculated and compared with determine whether there was a statistically significant difference between treatments. The significance level was set at $\alpha = 0.01$ to control for the overall type I error rate when doing multiple comparisons. The results of the above regression are transformed back into their original units (31).

Results

Selection, design, and characterization of peptides

The crystal structure of the Fab of pertuzumab bound to the ECD of HER-2/*neu* (22) reveals that pertuzumab binds to HER-2/*neu* in

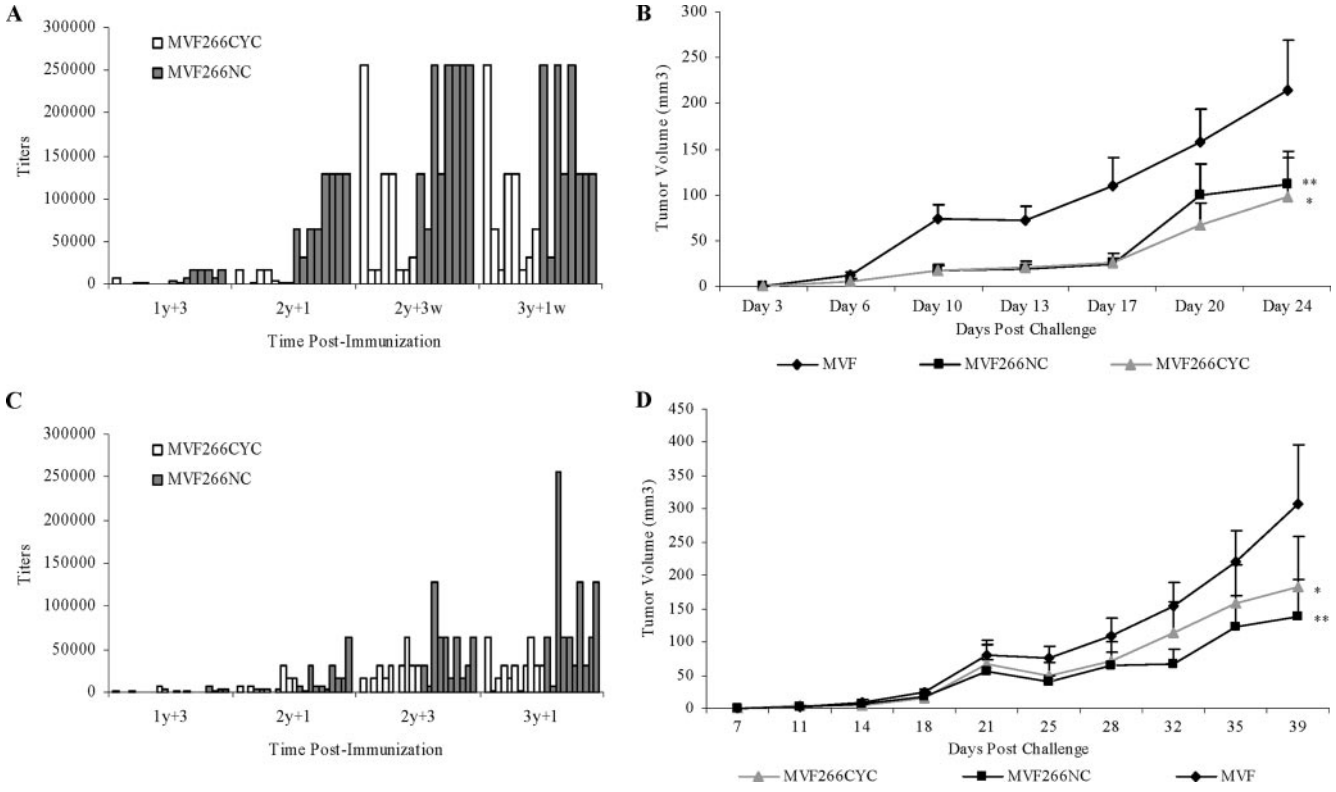

FIGURE 5. In vivo suppression of transplantable tumor growth by active immunization with MVF266 peptide epitopes. *A*, FVB/n mice were immunized with MVF266CYC, MVF266NC, or MVF ($n = 8$) three times (as described in *Materials and Methods*) and immunogenicity was determined by ELISA. Each bar represents the titers of individual mouse. Ab titers are defined as in the rabbit studies (Fig. 2). Ten days after the third immunization, mice were challenged with 3×10^6 NT2.5 cells s.c. *B*, Tumor size was monitored twice weekly for a total of 24 days. Results are reported as average tumor size (mm^3) + SEM. *, $p = <0.001$; **, $p = 0.002$. *C*, Immunogenicity of peptide vaccines determined in inbred BALB/c mice ($n = 10$). Fourteen days after the third immunization, mice were challenged with 1×10^5 TUBO cells s.c. *D*, Tumor size was monitored twice weekly for a total of 39 days. Results are reported as average tumor size (mm^3) + SEM. *, $p = 0.0007$; **, $p = 0.0002$.

subdomain II of the HER-2 ECD. Subdomain II contains an extensive disulfide-bonding network with seven disulfide-bonded modules. Within the central disulfide-bonded module is a β-hairpin (residues 269–288) that extends beyond the rest of the protein. Each epidermal growth factor receptor (EGFR) monomer contains this same β-hairpin extension, where it forms one side of the dimerization interface (32, 33). The 266–333 region of HER-2 was selected for the design of peptides with the objective of eliciting Abs against the peptides capable of inhibiting dimerization of HER-2 with other members of the EGFR family. We examined three different sequences, 266–296, 298–333, and 315–333 to determine the best minimal conformational epitope for effective B cell immunization (Table I). The 266–296 sequence contains the β-hairpin loop as well as four residues that contain atoms which directly contact pertuzumab atoms (as indicated by bold residues in Table I). The 298–333 sequence contains 7 aa which contact pertuzumab, whereas the 315–333 sequence has four residues in contact with pertuzumab. Although the 266–296 contains the β-hairpin loop that protrudes from the protein and is involved in heterodimerization, residues in 298–333 and 315–333 (Ser^{310}, Leu^{317}, and His^{318}) are essential for pertuzumab binding HER-2 based on mutagenesis studies (22). The correct disulfide pairings were achieved by selective side chain protection. For the 266–296 and 315–333 peptides, the side chain trityl was removed, and the disulfide bridge formed by I_2 oxidation in acetic acid (266–296, $M+H^+$ Cal/Obs 5759/5760; 315–333, $M+H^+$ Cal/Obs 4493/4495). The two disulfide bonds in the 298–333 peptide were achieved ($M+H^+$ Cal/Obs 6278/6280) as previously described (26).

CD measurements of measles virus fusion protein (MVF) 266–296 peptide

All peptides in the present study contain the MVF promiscuous T cell epitope sequence (282–302) attached with the four-residue turn sequence GPSL and the B cell sequence from the HER-2 protein. This peptide construct is a complex peptide in terms of its secondary structure elements. The rationale behind the design of these peptide constructs was to have independent folding of the MVF and B cell epitope to generate a specific B cell immune response. The protective peptide constructs MVF266 CYC and NC were studied at a concentration of 100 μM in water. Previous CD studies (34) of disulfide-bonded peptides indicated negative CD minimum at 217 nm and a positive maximum of 205 nm, suggesting that the peptide adopts a high degree of β-sheet conformation in addition to a small amount of type-II β-turn. The MVF266CYC construct is partially folded because of conformational constrains imposed by the disulfide bond in the B cell epitope. CD measurements at 100 μM show three minima at 193, 197, and 199 nm indicating a population of turn segments in this peptide construct. The MVF266NC construct shows minima at 195, 199, and 201 nm, indicating a different topology of the B cell epitope lacking constraints due to disulfide bonds. Neither peptide shows characteristic CD minima of the β-sheet structure. This is in agreement with the rationale of our peptide design, which is intended to have independent folding of the MVF and B cell epitopes within the peptide construct. CD studies (data not shown) suggest the presence of isolated β-turns and different secondary structure elements in the disulfide-bonded peptide construct.

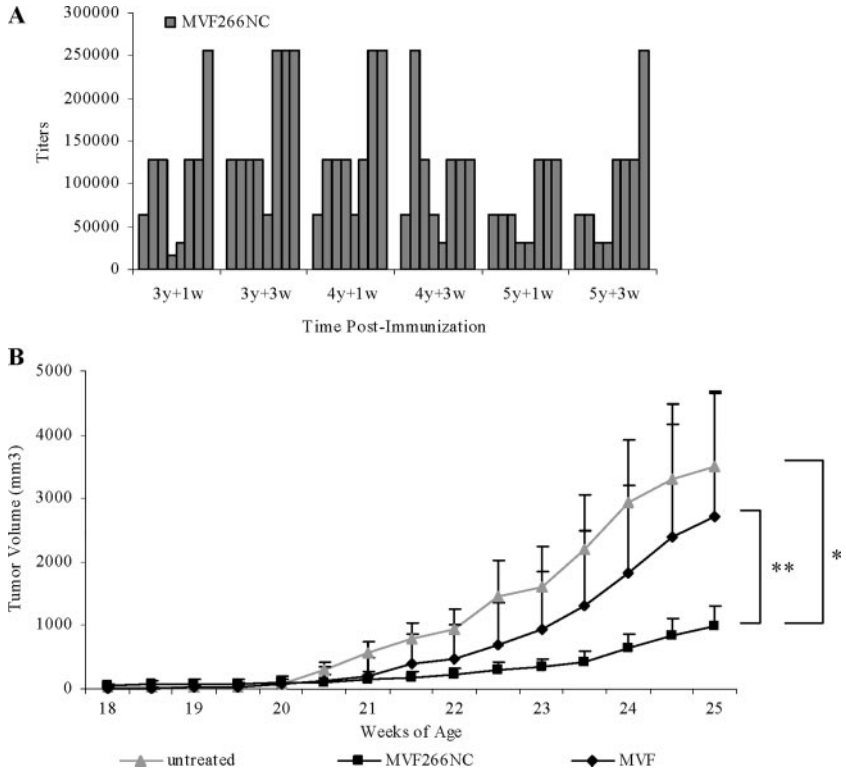

FIGURE 6. In vivo suppression of autochthonous tumor growth by active immunization with MVF 266 peptide epitope. BALB-*neu*T mice (n = 5–8) were immunized with MVF, MVF266NC, or left untreated. Beginning at 5–6 wk of age, mice were treated five times at 3- to 4-wk intervals. *A*, Immunogenicity of the MVF266NC construct in BALB-*neu*T mice. *B*, Tumor measurements were performed twice a week on each of 10 mammary glands. The data are presented as the average tumor size (mm^3) + SEM. *, $p = 0.0067$; **, $p = 0.0068$.

Immunogenicity of the constructs

Extremely high Ab titers (250,000–500,000) were obtained in rabbits immunized with both MVF266CYC and MVF266NC (Fig. 1*A*). Rabbits immunized with MVF298CYC and MVF298NC also elicited high titers (60,000–130,000) (Fig. 1*B*). Rabbits immunized with the MVF315CYC or MVF315NC construct elicited slightly lower titers (40,000–60,000), most probably due to the smaller size of the construct (Fig. 1*C*). The predominant isotype generated from all peptides was IgG (>95%), whereas IgM and IgA Abs were <5% of total Ig (Fig. 1*D*). The ability of the MVF266 peptide constructs to elicit the highest titer Abs indicates that this sequence was the most immunogenic.

*Cross-reactivity of the peptide Abs with the native HER-2/*neu *receptor*

Binding of the intact HER-2/*neu* receptor was determined by immunofluorescence staining of a single-cell suspension of BT474 (HER-2^{high}) cells. Differential binding was observed for each construct at 5 μg. Abs elicited by both MVF266CYC and MVF266NC bound the receptor similar to the control HER-2-specific humanized mAb trastuzumab (Fig. 2*A*, *left panel*). Abs to the MVF298CYC construct bound just within one log of trastuzumab, while the MVF298NC Abs did not exhibit any HER-2 protein binding (Fig. 2*B*, *left panel*). MVF315Cyc Abs bound within one log of trastuzumab and MVF315NC induced Abs did not bind (Fig. 2*C*, *left panel*). No binding was observed with the MDA468 cell line, a non-HER-2-overexpressing breast cancer cell line (Fig. 2, *A–C*, *right panel*). An indirect ELISA using SKBR-3 (HER-2^{high}) cell lysates was also used to determine the antipeptide Abs ability to bind the native receptor in comparison to the positive control rabbit polyclonal Ab, Ab-1 (Fig. 2*D*). MVF266CYC and MVF266NC Ab binding confirmed the flow cytometry data, exhibiting the highest absorbance with the cyclic peptide binding strongly, suggesting that the cyclized epitope may better mimic the corresponding site on the native HER-2/*neu* protein. In contrast, both the MVF298CYC and MVF298NC Abs bound with the next highest absorbance, while MVF315CYC and MVF315NC Abs bound with the lowest absorbance. The results of these studies show that of the six constructs, the MVF266 peptide Abs exhibited the strongest binding to the native receptor, indicating that this construct most closely mimics the secondary structure of the native receptor.

Antitumor activity of peptide Abs

We next tested the ability of the peptide Abs to mediate ADCC using human PBMCs as effector cells (35, 36). Both MVF266CYC and MVF266NC (50 μg) induced Abs showed high levels of dose-dependent cell lysis with E:T of 20:1 showing between 60 and 65% lysis as compared with the positive control trastuzumab with 75% lysis. MVF315CYC Abs induced 46% cell lysis, while MVF315NC, MVF298CYC and MVF298NC Abs did not exhibit lysis levels over background (Fig. 3*A*). The ADCC assay results correlate with the ability of the Abs against MVF266CYC, MVF266NC, and MVF315CYC to bind the native receptor in vitro indicating that these Abs not only bind the native receptor, but are able to effectively mediate antitumor activity.

Phosphorylation inhibition

The main mode of action of pertuzumab is the interruption of HER-2/*neu* dimerization with other members of the ErbB receptor family. To determine whether our peptide Abs disrupt dimerization and consequently phosphorylation of the receptor cytoplasmic tyrosine kinase regions, we used a phospho-HER-2 ELISA. SKBR-3 (HER-2^{high}) cells were treated with Ab and HRG (used to activate HER-3) before being lysed. Cell lysates were captured with an anti-HER-2 mAb and probed with a phospho-HER-2 Ab. Both MVF266CYC (51.4%) and MVF266NC (55.2%) Abs and to a slightly lesser extent MVF315CYC Abs (47.1%) lowered the concentration of phosphotyrosine on SKBR-3 cells as compared with the control HER-2/*neu* phosphorylation inhibitor, AG825 (64.9%)

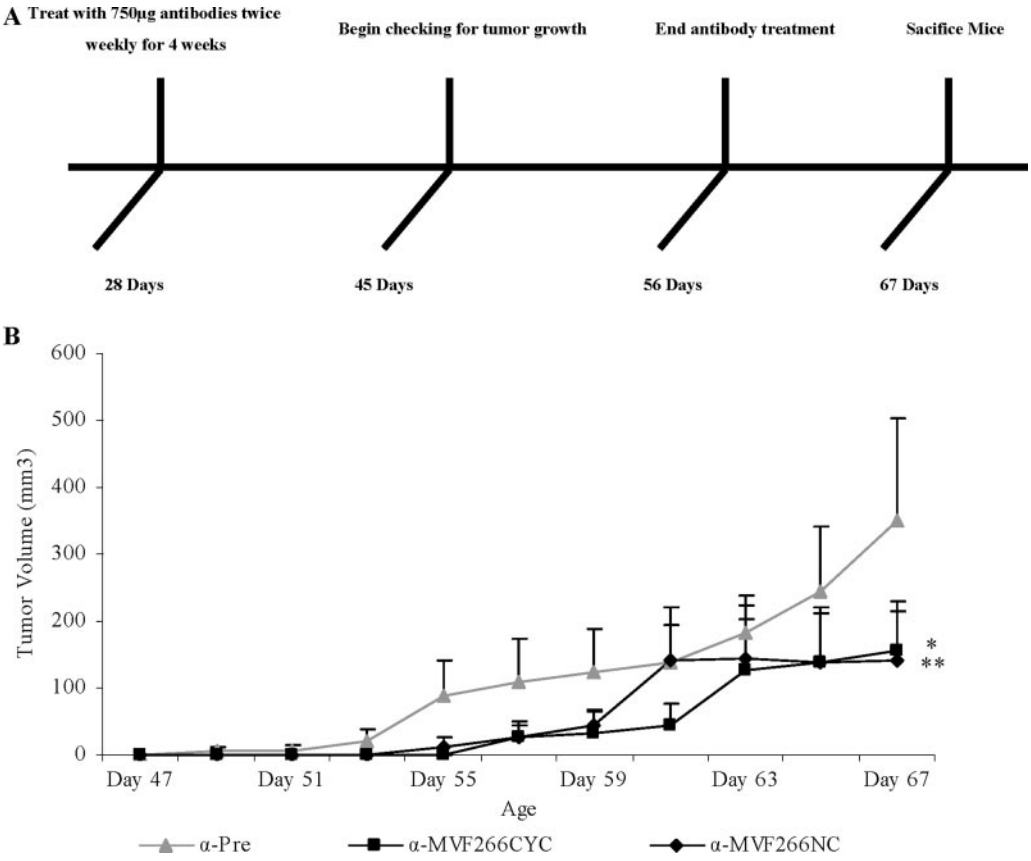

FIGURE 7. In vivo suppression of autochthonous tumor growth by passive immunization with purified rabbit anti-peptide Abs (anti-MVF266 CYC and anti-MVF266NC). A surrogate model of vaccination in VEGF$^{+/-}$Neu2–5$^{+/-}$ mice, which develop tumors at an average of 56 days, was used. *A*, Each group ($n = 10$) was treated twice weekly with 750 μg of purified rabbit anti-peptide Abs (anti-MVF266 CYC and anti-MVF266NC) for 4 wk. Mice were monitored for tumor development starting at 45 days of age. Mice were sacrificed at 67 days of age. *B*, Results are reported as average tumor size (mm^3) + SEM. *, $p = 0.0001$; **, $p = 0.0008$.

(Fig. 3*B*). The reduction in phosphotyrosine indicates that these Abs are capable of inhibiting phosphorylation of the tyrosine kinase domains due to blockade of the extracellular HER-2/*neu* dimerization loop. We conclude Abs to both the MVF266 constructs were effective in blocking the dimerization of HER-2/*neu*.

Antiproliferative effects of peptide Abs

The antiproliferative effects of the MVF266CYC and MVF266NC Abs were tested on MCF-7 (HER-2^{low}) cells in the presence of HRG to activate the HER-3 receptor. It is known that pertuzumab acts on cells by disrupting ligand-dependent receptor complexes independent of HER-2/*neu* expression (37). Serum-starved MCF-7 cells were incubated with Abs before HRG exposure. We found that both MVF266CYC and MVF266NC Abs inhibited tumor growth (23.4 and 13.2% inhibition, respectively) at a concentration of 50 μg/ml, with MVF266CYC Abs more efficiently inhibiting proliferation (data not shown). Normal rabbit IgG did not show antiproliferative activity.

Transplantable tumor challenge models

To determine the ability of the MVF266 peptide vaccine candidates to inhibit the formation of tumors in vivo, we studied two different rat *neu*-expressing tumor challenge models. There is 97% sequence homology between human HER-2 and rat *neu* within the human HER-2 266–296 sequence with only one disparate amino acid (Fig. 4*A*). We performed flow cytometry to determine whether MVF266 anti-peptide Abs were cross-reactive with rat *neu* using NT2.5 cells (isolated from FVB/n202 *neu*$^+$ tumors) (38). Abs raised against both MVF266CYC and MVF266NC (5 μg) were shifted relative to isotype control IgG and bound the receptor similar to the control *neu*-specific Ab Ab-4 (Fig. 4*B*).

Preliminary studies determined minimum rejection time in untreated animals, allowing us to limit our studies to the growth phase of tumor development. FVB/n mice ($n = 8$) were immunized with MVF266CYC, MVF266NC peptide constructs and MVF alone as the negative control. Titers (Fig. 5*A*) were monitored weekly to determine the immunogenicity of the constructs in mice. Ten days after the third immunization, the mice were challenged with 3×10^6 NT2.5 cells. High-titer Abs to MVF266–296CYC and MVF266–296NC were observed by the end of the study. MVF-specific Abs were not detectable in MVF-immunized control FVB/n mice.

The mean tumor volumes in the MVF266 treatment groups are shown in Fig. 5*B*. There was a significant difference between the tumor burden of mice immunized with MVF266CYC or MVF266NC vs MVF-immunized controls ($p = <0.001$ and $p = 0.002$, respectively) that indicates both peptide vaccine constructs were protective.

To further investigate the efficacy of the MVF266 vaccine peptides, we challenged BALB/c mice with TUBO cells derived from tumors of BALB-*neu*T transgenic mice (39) which is a more aggressive tumor model. Groups of BALB/c mice ($n = 10$) were immunized with MVF266CYC, MVF266NC, or MVF and Ab titers monitored on a weekly basis. Lower titers were observed in the BALB/c mice as compared with the FVB/n mice, and no MVF-specific Abs were detectable in immunized control mice (Fig. 5*C*).

The mean tumor volumes over time for each of the three treatment groups are shown in Fig. 5*D*. Statistical significance was found between mice immunized with MVF vs mice immunized with MVF266CYC or MVF266NC ($p = 0.0002$ and $p = 0.0007$, respectively), which confirms that immunization of mice with either MVF266CYC or MVF266NC reduces tumor burden. We conclude that the MVF266 peptide constructs are effective in eliciting protective immune responses by generating high titer Abs that bind the native HER-2/*neu* receptor and inhibit the growth and differentiation of cancerous cells.

Effect of peptide vaccines on autochthonous mammary carcinomas

The BALB-*neu*T mouse model is likely the most aggressive model of *neu*-induced carcinogenesis and was used as a measure of the ability of the peptide constructs to reduce tumor progression (23). Animals rapidly develop tumors; in preliminary studies, 100% of untreated mice developed tumors by 25 wk of age. The MVF266NC epitope elicited high-titer Ab responses 3 wk after the third immunization (Fig. 6*A*). Mice immunized with MVF266NC had a significant reduction in tumor volume ($p = 0.0068$) as compared with mice immunized with MVF or left untreated ($p = 0.0067$) (Fig. 6*B*).

Effect of a surrogate vaccine model on autochthonous mammary carcinomas

The VEGF$^{+/-}$Neu2–5$^{+/-}$ mouse model has an activating mutation of the *neu* gene coupled with the overexpression of the angiogenic factor vascular endothelial growth factor (VEGF) (25). These mice quickly develop tumors at ~56 days of age, which does not allow time for conventional immunization and Ab response to develop before tumor onset. To circumvent this issue, mice were passively injected with rabbit purified anti-peptide Abs to both the MVF266 constructs (see Fig. 1*A*) twice weekly for 4 wk to simulate development of Abs in vivo (Fig. 7*A*). We found that MVF266CYC and MVF266NC Abs suppressed tumor formation, showing statistically significant reduction ($p = 0.0001$ and $p = 0.0008$, respectively) in tumor development as compared with the IgG-treated mice (Fig. 7*B*). Both Abs to the MVF 266 are effective in inhibiting the growth of cancerous cells.

Discussion

The HER-2/*neu* protein has become a target for cancer therapy as it is overexpressed in a significant fraction of breast cancers. Patients with HER-2/*neu*-overexpressing tumors have shown the ability to mount weak immune responses to this Ag, indicating that HER-2/*neu* is immunogenic. In addition, the HER-2/*neu* receptor is exposed to the extracellular matrix making it available for direct Ab binding. Trastuzumab, a humanized mAb, was one of the first target-specific molecules to be successfully exploited for clinical use (40). Recent studies have demonstrated significant improvements in disease-free survival of women with early stage HER-2-positive breast cancer when trastuzumab was combined with adjuvant chemotherapy (41, 42). Pertuzumab, another humanized mAb, is also a HER-2/*neu* inhibitor that has a different mechanism of action from trastuzumab. Pertuzumab binds to the dimerization loop in the ECD domain of HER-2/*neu*, preventing HER-2/*neu* from interacting with other members of the ErbB family, thus blocking transphosphorylation of the tyrosine kinase domains on the intracellular tails of the receptors and further signal transduction.

There are a number of issues with the use of passive cancer immunotherapy including the requirement for repeated dosing and its high cost, the development of resistance through loss of immunodominant epitopes and undesired immunogenicity of humanized and chimerized Abs. A vaccine would trigger the body to produce its own Abs which has several advantages, some of which include less immunogenicity as well as sustained immune response due to long-term immunologic memory. There have been many studies with peptide cancer vaccines, the majority of which target the cellular arm of the immune system by activating CD8$^+$ CTL. To date, most of the HER-2/*neu*-specific peptide vaccines have been restricted to T cell epitopes. Disis et al. (43, 44), vaccinated patients with HER-2/*neu*-overexpressing tumors with a mixture of the CTL peptides HER-2(p369–384), HER-2(p688–703), and HER-2(p971–984) admixed with GM-CSF. Ninety-two percent of the patients developed a T cell response to the peptides, with a preferential response directed against the HER-2(p369–384) epitope, and 38% of the patients continued to show immunity 1 year later (43, 44). This and other similar clinical trials proved that peptides can be used to effectively immunize against HER-2/*neu*. One of the major drawbacks of T cell-based vaccines is the restricted applicability due to MHC haplotype specificity (21).

Our laboratory has focused on the humoral arm of the immune system by creating vaccines that combine a molecularly defined B cell epitope with a "promiscuous" Th-activating epitope. Our work has focused on the identification, characterization, and evaluation of the B cell epitope of the ECD domain of HER-2/*neu* oncoprotein. Recently, we examined the effect of conformationally constraining an epitope from near the trastuzumab-binding region of HER-2/*neu* and found that the cyclized, conformational epitope enhanced antitumor activity (26). Our ongoing efforts to enhance Ab affinity and cross-reactivity have led us to investigate whether constraining the dimerization loop peptide with the native disulfide bonds would enhance the affinity of the Abs and consequently its biological in vivo efficacy.

Pertuzumab has shown activity in reducing cellular proliferation, signal transduction, and tumor growth in xenograft models (10, 37, 45). We identified three peptide epitopes (266–296, 298–333, 315–333) that mimic the dimerization loop of the HER-2/*neu* receptor and used them for vaccines to induce endogenous Abs to this region. The immunogenicity of the disulfide-bonded (CYC) and linear (NC) peptides were evaluated in rabbits. High Ab titers were elicited with MVF266CYC, MVF266NC, MVF298CYC, and MVF298NC vaccine constructs. Lower titers were seen in rabbits immunized with MVF315CYC and MVF315NC, presumably due to the small size of the epitope. The Abs generated were tested by flow cytometry and we found that both the MVF266 constructs bound to HER-2-expressing cells with the cyclized form binding slightly better than the NC form. The MVF315CYC construct showed strong binding to the cognate receptor, while the MVF298CYC, MVF298NC, and MVF315NC constructs showed weak or no binding. These findings were further supported by the results of testing the antitumor effects of the Abs by ADCC. MVF266CYC, MVF266NC, and MVF315CYC all showed HER-2-specific cell lysis, while the other three constructs did not produce tumor lysis above background levels. Interestingly, when the Abs were tested for binding to the native receptor in cell lysates, both the MVF298 constructs showed stronger binding than both of the MVF315 constructs did. This could be attributed to the native protein not being tested in intact cells, but in cellular lysates which could have either modified the conformation of the receptor or exposed additional binding sites in the intracellular and transmembrane regions.

We evaluated the MVF266CYC, MVF266NC, and MVF315CYC Abs in vitro, as they had shown the greatest anti-HER-2/*neu* activity. We determined that our Abs block cytoplasmic phosphorylation in HER-2/*neu*-expressing cells and indirectly receptor dimerization. This confirms previous results testing the ability of pertuzumab to block

HRG-induced tyrosine phosphorylation as detected by Western blots (37, 46). MVF266CYC and MVF266NC also showed the ability to block HRG-activated proliferation in cells expressing physiological levels of HER-2/*neu*, similar to previous results (37, 45).

We used two tumor challenge models in which mice were immunized before being challenged with syngeneic tumor lines. Immunization with MVF266CYC and MVF266NC significantly inhibited tumor growth in both models. In addition, we tested the vaccine constructs in two transgenic autochthonous tumor models of breast cancer, which are more clinically relevant than challenge models as they actually go through the process of tissue transformation and tumor development without external manipulations. Both active immunization of BALB-*neu*T mice with the MVF266 peptide constructs and a surrogate passive vaccination model in VEGF$^{+/-}$Neu2–5$^{+/-}$ mice with purified rabbit Abs to the MVF266 peptide constructs resulted in a reduction of tumor burden in treated mice as compared with control mice. The results from these models echo the results found by other groups testing the ability of dimerization blockers to reduce tumor growth in vivo (37, 46). The mouse Ab isotype distribution is similar for protective peptides (MVF266CYC and NC) and nonprotective peptides (MVF298CYC and NC, MVF315CYC, and NC). IgG2a accounted for 32–45% of total Ig, an isotype associated with an effective antitumor response (39, 47, 48). The same relative isotype distribution between protective and nonprotective peptides indicates that efficacy of the vaccine was due to the affinity of the anti-peptide Abs for the HER-2 dimerization interface.

There was a reduction in tumor burden but not complete protection of animals vaccinated with the MVF266 peptide constructs or treated with anti-MVF266 Abs using both syngeneic tumor transplants and transgenic mice. We do not believe that residual tumor growth is due to a lack of affinity of the Abs to HER-2/*neu* based on binding studies of anti-266 Abs to HER-2 (Fig. 2). Tumors present many barriers for endogenous Abs to gain access including heterogenous vascularization and high interstitial fluid pressure, opposing convection and diffusion. Thus, residual tumor growth could be due to the anti-peptide Abs inability to access all tumor cells. Alternatively, the residual tumor growth could be due to resistance of cells to HER-2/*neu*-targeted therapy. Trastuzumab resistance has been attributed to increased signaling by the PI3K/Akt pathway as well as loss of function of the tumor suppressor *PTEN* gene, the negative regulator of Akt (49). These mechanisms of resistance could explain the residual tumor growth. Additionally, of importance is that both the BALB-*neu*T and VEGF$^{+/-}$Neu2–5$^{+/-}$ models are extremely aggressive models of rat HER-2/*neu* carcinogenesis. Both these transgenic models use the mouse mammary tumor virus promoter, an extremely potent promoter targeting the transgenes for mammary glands. Residual tumor growth can also be attributed to the particularly aggressive nature of these models.

Our studies indicate the 266–296 epitope peptide holds the most promise as a prophylactic vaccine against HER-2/*neu*-expressing breast cancer. Results show that while conformational restraints do not necessarily lead to enhanced antitumor effects for this specific construct, the ability of MVF315CYC to better bind the native protein and mediate ADCC activity as well as previous results (26) indicate that conformation is important for some epitopes. It is possible that the MVF266NC construct folds in a similar conformation to the MVF266CYC peptide even without the disulfide bridge, while other constructs require the conformational constraint to more closely mimic the native protein. Given the mode of action of pertuzumab in that it sterically interferes with HER-2 dimerization and signaling pathways, it is expected that the 266–296 construct could be effective in both HER-2-overexpressing cancers as well as normal HER-2-expressing cancers such as lung, ovarian, and colon. Pertuzumab is being investigated in clinical trials in patients whose tumors do not contain the amplified ErbB2 gene because pertuzumab inhibits the dimerization of HER-2 with EGFR and HER-3. Thus, our vaccine targeting the dimerization arm of HER-2 could be efficacious in patients who do not overexpress HER-2 but have normal expression. Although the mechanisms by which Abs exert their therapeutic effects are still being debated, the putative mechanisms are either direct (i.e., block signaling functions, internalization of receptors, reduce proteolytic cleavage of receptors) or indirect action mediated by the immune system (complement-dependent cytotoxicity, ADCC). For future studies, we plan to investigate in detail the mechanism of action of the anti-peptide Abs including the effect of downstream proteins of HER-2 including Akt and MAPK. Additionally, such studies will also include combination vaccine therapy in which 266–296 will be added to epitopes from the trastuzumab-binding site to determine whether there is an additive/synergistic effect on antitumor capabilities.

Disclosures

The authors have no financial conflict of interest.

References

1. Coussens, L., T. L. Yang-Feng, Y. C. Liao, E. Chen, A. Gray, J. McGrath, P. H. Seeburg, T. A. Libermann, J. Schlessinger, U. Francke, et al. 1985. Tyrosine kinase receptor with extensive homology to EGF receptor shares chromosomal location with *neu* oncogene. *Science* 230: 1132–1139.
2. Yarden, Y., and J. Schlessinger. 1987. Epidermal growth factor induces rapid, reversible aggregation of the purified epidermal growth factor receptor. *Biochemistry* 26: 1443–1451.
3. Stern, D. F., and M. P. Kamps. 1988. EGF-stimulated tyrosine phosphorylation of p185*neu*: a potential model for receptor interactions. *EMBO J.* 7: 995–1001.
4. Wada, T., X. L. Qian, and M. I. Greene. 1990. Intermolecular association of the p185*neu* protein and EGF receptor modulates EGF receptor function. *Cell* 61: 1339–1347.
5. Slamon, D. J., G. M. Clark, S. G. Wong, W. J. Levin, A. Ullrich, and W. L. McGuire. 1987. Human breast cancer: correlation of relapse and survival with amplification of the HER-2/*neu* oncogene. *Science* 235: 177–182.
6. Gusterson, B. A., R. D. Gelber, A. Goldhirsch, K. N. Price, J. Save-Soderborgh, R. Anbazhagan, J. Styles, C. M. Rudenstam, R. Golouh, R. Reed, et al. 1992. Prognostic importance of c-erbB-2 expression in breast cancer. International (Ludwig) Breast Cancer Study Group. *J. Clin. Oncol.* 10: 1049–1056.
7. Andrulis, I. L., S. B. Bull, M. E. Blackstein, D. Sutherland, C. Mak, S. Sidlofsky, K. P. Pritzker, R. W. Hartwick, W. Hanna, L. Lickley, et al. 1998. *neu*/erbB-2 amplification identifies a poor-prognosis group of women with node-negative breast cancer. Toronto Breast Cancer Study Group. *J. Clin. Oncol.* 16: 1340–1349.
8. Cobleigh, M. A., C. L. Vogel, D. Tripathy, N. J. Robert, S. Scholl, L. Fehrenbacher, J. M. Wolter, V. Paton, S. Shak, G. Lieberman, and D. J. Slamon. 1999. Multinational study of the efficacy and safety of humanized anti-HER2 monoclonal antibody in women who have HER2-overexpressing metastatic breast cancer that has progressed after chemotherapy for metastatic disease. *J. Clin. Oncol.* 17: 2639–2648.
9. Fendly, B. M., M. Winget, R. M. Hudziak, M. T. Lipari, M. A. Napier, and A. Ullrich. 1990. Characterization of murine monoclonal antibodies reactive to either the human epidermal growth factor receptor or HER2/*neu* gene product. *Cancer Res.* 50: 1550–1558.
10. Jackson, J. G., P. St. Clair, M. X. Sliwkowski, and M. G. Brattain. 2004. Blockade of epidermal growth factor- or heregulin-dependent ErbB2 activation with the anti-ErbB2 monoclonal antibody 2C4 has divergent downstream signaling and growth effects. *Cancer Res.* 64: 2601–2609.
11. Gordon, M. S., D. Matei, C. Aghajanian, U. A. Matulonis, M. Brewer, G. F. Fleming, J. D. Hainsworth, A. A. Garcia, M. D. Pegram, R. J. Schilder, et al. 2006. Clinical activity of pertuzumab (rhuMAb 2C4), a HER dimerization inhibitor, in advanced ovarian cancer: potential predictive relationship with tumor HER2 activation status. *J. Clin. Oncol.* 24: 4324–4332.
12. Agus, D. B., M. S. Gordon, C. Taylor, R. B. Natale, B. Karlan, D. S. Mendelson, M. F. Press, D. E. Allison, M. X. Sliwkowski, G. Lieberman, et al. 2005. Phase I clinical study of pertuzumab, a novel HER dimerization inhibitor, in patients with advanced cancer. *J. Clin. Oncol.* 23: 2534–2543.
13. Slamon, D. J., B. Leyland-Jones, S. Shak, H. Fuchs, V. Paton, A. Bajamonde, T. Fleming, W. Eiermann, J. Wolter, M. Pegram, et al. 2001. Use of chemotherapy plus a monoclonal antibody against HER2 for metastatic breast cancer that overexpresses HER2. *N. Engl. J. Med.* 344: 783–792.
14. Disis, M. L., E. Calenoff, G. McLaughlin, A. E. Murphy, W. Chen, B. Groner, M. Jeschke, N. Lydon, E. McGlynn, R. B. Livingston, et al. 1994. Existent T-cell and antibody immunity to HER-2/*neu* protein in patients with breast cancer. *Cancer Res.* 54: 16–20.

15. Disis, M. L., S. M. Pupa, J. R. Gralow, R. Dittadi, S. Menard, and M. A. Cheever. 1997. High-titer HER-2/*neu* protein-specific antibody can be detected in patients with early-stage breast cancer. *J. Clin. Oncol.* 15: 3363–3367.
16. Kiessling, R., W. Z. Wei, F. Herrmann, J. A. Lindencrona, A. Choudhury, K. Kono, and B. Seliger. 2002. Cellular immunity to the Her-2/*neu* protooncogene. *Adv. Cancer Res.* 85: 101–144.
17. Baxevanis, C. N., N. N. Sotiriadou, A. D. Gritzapis, P. A. Sotiropoulou, S. A. Perez, N. T. Cacoullos, and M. Papamichail. 2006. Immunogenic HER-2/*neu* peptides as tumor vaccines. *Cancer Immunol. Immunother.* 55: 85–95.
18. Disis, M. L., J. R. Gralow, H. Bernhard, S. L. Hand, W. D. Rubin, and M. A. Cheever. 1996. Peptide-based, but not whole protein, vaccines elicit immunity to HER-2/*neu*, oncogenic self-protein. *J. Immunol.* 156: 3151–3158.
19. Disis, M. L., K. H. Grabstein, P. R. Sleath, and M. A. Cheever. 1999. Generation of immunity to the HER-2/*neu* oncogenic protein in patients with breast and ovarian cancer using a peptide-based vaccine. *Clin. Cancer Res.* 5: 1289–1297.
20. Dakappagari, N. K., D. B. Douglas, P. L. Triozzi, V. C. Stevens, and P. T. Kaumaya. 2000. Prevention of mammary tumors with a chimeric HER-2 B-cell epitope peptide vaccine. *Cancer Res.* 60: 3782–3789.
21. Dakappagari, N. K., J. Pyles, R. Parihar, W. E. Carson, D. C. Young, and P. T. Kaumaya. 2003. A chimeric multi-human epidermal growth factor receptor-2 B cell epitope peptide vaccine mediates superior antitumor responses. *J. Immunol.* 170: 4242–4253.
22. Franklin, M. C., K. D. Carey, F. F. Vajdos, D. J. Leahy, A. M. de Vos, and M. X. Sliwkowski. 2004. Insights into ErbB signaling from the structure of the ErbB2-pertuzumab complex. *Cancer Cell.* 5: 317–328.
23. Boggio, K., G. Nicoletti, E. Di Carlo, F. Cavallo, L. Landuzzi, C. Melani, M. Giovarelli, I. Rossi, P. Nanni, C. De Giovanni, et al. 1998. Interleukin 12-mediated prevention of spontaneous mammary adenocarcinomas in two lines of Her-2/*neu* transgenic mice. *J. Exp. Med.* 188: 589–596.
24. Siegel, P. M., E. D. Ryan, R. D. Cardiff, and W. J. Muller. 1999. Elevated expression of activated forms of Neu/ErbB-2 and ErbB-3 are involved in the induction of mammary tumors in transgenic mice: implications for human breast cancer. *EMBO J.* 18: 2149–2164.
25. Oshima, R. G., J. Lesperance, V. Munoz, L. Hebbard, B. Ranscht, N. Sharan, W. J. Muller, C. A. Hauser, and R. D. Cardiff. 2004. Angiogenic acceleration of Neu induced mammary tumor progression and metastasis. *Cancer Res.* 64: 169–179.
26. Dakappagari, N. K., K. D. Lute, S. Rawale, J. T. Steele, S. D. Allen, G. Phillips, R. T. Reilly, and P. T. Kaumaya. 2005. Conformational HER-2/*neu* B-cell epitope peptide vaccine designed to incorporate two native disulfide bonds enhances tumor cell binding and antitumor activities. *J. Biol. Chem.* 280: 54–63.
27. Sundaram, R., M. P. Lynch, S. V. Rawale, Y. Sun, M. Kazanji, and P. T. Kaumaya. 2004. De novo design of peptide immunogens that mimic the coiled coil region of human T-cell leukemia virus type-1 glycoprotein 21 transmembrane subunit for induction of native protein reactive neutralizing antibodies. *J. Biol. Chem.* 279: 24141–24151.
28. Soll, R., and A. G. Beck-Sickinger. 2000. On the synthesis of orexin A: a novel one-step procedure to obtain peptides with two intramolecular disulphide bonds. *J. Pept. Sci.* 6: 387–397.
29. Chen, Y. H., J. T. Yang, and K. H. Chau. 1974. Determination of the helix and β form of proteins in aqueous solution by circular dichroism. *Biochemistry* 13: 3350–3359.
30. Greenfield, N., and G. D. Fasman. 1969. Computed circular dichroism spectra for the evaluation of protein conformation. *Biochemistry* 8: 4108–4116.
31. Zeger, S. L., K. Y. Liang, and P. S. Albert. 1988. Models for longitudinal data: a generalized estimating equation approach. *Biometrics* 44: 1049–1060.
32. Garrett, T. P., N. M. McKern, M. Lou, T. C. Elleman, T. E. Adams, G. O. Lovrecz, H. J. Zhu, F. Walker, M. J. Frenkel, P. A. Hoyne, et al. 2002. Crystal structure of a truncated epidermal growth factor receptor extracellular domain bound to transforming growth factor α. *Cell* 110: 763–773.
33. Ogiso, H., R. Ishitani, O. Nureki, S. Fukai, M. Yamanaka, J. H. Kim, K. Saito, A. Sakamoto, M. Inoue, M. Shirouzu, and S. Yokoyama. 2002. Crystal structure of the complex of human epidermal growth factor and receptor extracellular domains. *Cell* 110: 775–787.
34. Lakshminarayanan, R., E. O. Chi-Jin, X. J. Loh, R. M. Kini, and S. Valiyaveettil. 2005. Purification and characterization of a vaterite-inducing peptide, pelovaterin, from the eggshells of *Pelodiscus sinensis* (Chinese soft-shelled turtle). *Biomacromolecules* 6: 1429–1437.
35. Stancovski, I., E. Hurwitz, O. Leitner, A. Ullrich, Y. Yarden, and M. Sela. 1991. Mechanistic aspects of the opposing effects of monoclonal antibodies to the ERBB2 receptor on tumor growth. *Proc. Natl. Acad. Sci. USA* 88: 8691–8695.
36. Stockmeyer, B., T. Valerius, R. Repp, I. A. Heijnen, H. J. Buhring, Y. M. Deo, J. R. Kalden, M. Gramatzki, and J. G. van de Winkel. 1997. Preclinical studies with FcγR bispecific antibodies and granulocyte colony-stimulating factor-primed neutrophils as effector cells against HER-2/*neu* overexpressing breast cancer. *Cancer Res.* 57: 696–701.
37. Agus, D. B., R. W. Akita, W. D. Fox, G. D. Lewis, B. Higgins, P. I. Pisacane, J. A. Lofgren, C. Tindell, D. P. Evans, K. Maiese, et al. 2002. Targeting ligand-activated ErbB2 signaling inhibits breast and prostate tumor growth. *Cancer Cell.* 2: 127–137.
38. Reilly, R. T., M. B. Gottlieb, A. M. Ercolini, J. P. Machiels, C. E. Kane, F. I. Okoye, W. J. Muller, K. H. Dixon, and E. M. Jaffee. 2000. HER-2/*neu* is a tumor rejection target in tolerized HER-2/*neu* transgenic mice. *Cancer Res.* 60: 3569–3576.
39. Rovero, S., A. Amici, E. D. Carlo, R. Bei, P. Nanni, E. Quaglino, P. Porcedda, K. Boggio, A. Smorlesi, P. L. Lollini, et al. 2000. DNA vaccination against rat her-2/Neu p185 more effectively inhibits carcinogenesis than transplantable carcinomas in transgenic BALB/c mice. *J. Immunol.* 165: 5133–5142.
40. Pupa, S. M., E. Tagliabue, S. Menard, and A. Anichini. 2005. HER-2: a biomarker at the crossroads of breast cancer immunotherapy and molecular medicine. *J. Cell. Physiol.* 205: 10–18.
41. Piccart-Gebhart, M. J., M. Procter, B. Leyland-Jones, A. Goldhirsch, M. Untch, I. Smith, L. Gianni, J. Baselga, R. Bell, C. Jackisch, et al. 2005. Trastuzumab after adjuvant chemotherapy in HER2-positive breast cancer. *N. Engl. J. Med.* 353: 1659–1672.
42. Romond, E. H., E. A. Perez, J. Bryant, V. J. Suman, C. E. Geyer, Jr., N. E. Davidson, E. Tan-Chiu, S. Martino, S. Paik, P. A. Kaufman, et al. 2005. Trastuzumab plus adjuvant chemotherapy for operable HER2-positive breast cancer. *N. Engl. J. Med.* 353: 1673–1684.
43. Knutson, K. L., K. Schiffman, and M. L. Disis. 2001. Immunization with a HER-2/*neu* helper peptide vaccine generates HER-2/*neu* CD8 T-cell immunity in cancer patients. *J. Clin. Invest.* 107: 477–484.
44. Disis, M. L., T. A. Gooley, K. Rinn, D. Davis, M. Piepkorn, M. A. Cheever, K. L. Knutson, and K. Schiffman. 2002. Generation of T-cell immunity to the HER-2/*neu* protein after active immunization with HER-2/*neu* peptide-based vaccines. *J. Clin. Oncol.* 20: 2624–2632.
45. Takai, N., A. Jain, N. Kawamata, L. M. Popoviciu, J. W. Said, S. Whittaker, I. Miyakawa, D. B. Agus, and H. P. Koeffler. 2005. 2C4, a monoclonal antibody against HER2, disrupts the HER kinase signaling pathway and inhibits ovarian carcinoma cell growth. *Cancer* 104: 2701–2708.
46. Mendoza, N., G. L. Phillips, J. Silva, R. Schwall, and D. Wickramasinghe. 2002. Inhibition of ligand-mediated HER2 activation in androgen-independent prostate cancer. *Cancer Res.* 62: 5485–5488.
47. Nanni, P., L. Landuzzi, G. Nicoletti, C. De Giovanni, I. Rossi, S. Croci, A. Astolfi, M. Iezzi, E. Di Carlo, P. Musiani, et al. 2004. Immunoprevention of mammary carcinoma in HER-2/*neu* transgenic mice is IFN-γ and B cell dependent. *J. Immunol.* 173: 2288–2296.
48. Park, J. M., M. Terabe, Y. Sakai, J. Munasinghe, G. Forni, J. C. Morris, and J. A. Berzofsky. 2005. Early role of $CD4^+$ Th1 cells and antibodies in HER-2 adenovirus vaccine protection against autochthonous mammary carcinomas. *J. Immunol.* 174: 4228–4236.
49. Nahta, R., D. Yu, M. C. Hung, G. N. Hortobagyi, and F. J. Esteva. 2006. Mechanisms of disease: understanding resistance to HER2-targeted therapy in human breast cancer. *Nat. Clin. Pract. Oncol.* 3: 269–280.